

Activity Density Map Dis-similarity Comparison for Eldercare Monitoring

Shuang Wang, Marjorie Skubic *Member, IEEE*, and Yingnan Zhu *Student Member, IEEE*

Abstract—This paper describes ongoing work in analyzing sensor data logged in the homes of seniors. A visualization of motion sensor data in the form of a density map which uses different colors to show levels of activity was introduced previously. For evaluating changes in activity level and periodicity of life style, we introduce a dis-similarity measurement of density maps based on co-occurrence matrices. The dis-similarity between two density maps is captured using texture features for automatically determining changes in activity patterns. A case study is included to illustrate how the density map can be used to track activity patterns over time.

I. INTRODUCTION

BY the year 2030, the elderly population will double [1]. Technology that can help seniors “age in place” has highlighted in recent years, spurred by an aging population. response to this trend, many researchers have been investigating new approaches in caring for the elderly. One example of this research focus at the University of Missouri has resulted in TigerPlace (TP), an aging in place for seniors. Technologies to support independent living for older adults have been available for several years, such as [3][4][5][6][7]. Live-in laboratory smart homes with sensors and actuators have also been established such as the Aware Home at Georgia Tech[8] and MIT’s PlaceLab[9].

One focus of our research is the creation of intelligent software that uses sensors to uncover patterns of activity helpful to caregivers [2]. Sensor networks have been installed in 19 apartments in TP. Data collection has been ongoing for 2-3 years in some apartments. This is allowing us to study the data and develop algorithms for identifying alert conditions. The goal is to capture patterns representing physical and cognitive health conditions and then recognize when activity patterns begin to deviate from the norm.

In previous work [12], we focused on the visualization of motion activity density and time away from home (TAFH) the form of a density map that can be used to monitor the life style patterns of older adults. In a density map, different colors represent different levels of density in the motion sensor data, as shown in Fig.1. The density d is computed as the number of all motion sensor hits s during an hour divided by time at home during that hour, t . The density is defined as $= \frac{s}{t}$. The motion sensors generate events every 7 seconds if

continuous motion is detected. In lab tests, we have captured one-sensor density values ranging from 14 hits/hour for near motionless sitting to over 300 hits/hour for pacing. In Fig. 1, the X-axis shows hours in a day; the Y-axis shows days in a month. Black represents TAFH.

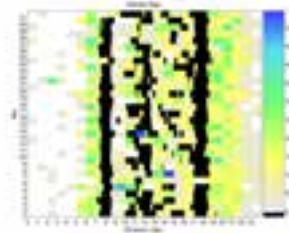


Fig.1. An example of a density map

In this paper, a dis-similarity measure based on texture features is proposed for comparing density maps and automatically determining changes in activity patterns. Although the activity density map is useful as a visualization for manual observation, we are also interested in automatically identifying changes in activity pattern. So we propose computing the dis-similarity between two density maps to aid caregivers in evaluating changes of residents. The concept of dis-similarity is fundamentally important in many applications and can be difficult to measure. Here, we propose using texture features to evaluate the dis-similarity of density maps by capturing spatial, frequency, and perceptual properties such as periodicity, coarseness, and complexity. Texture features are extracted using the co-occurrence distribution as described in Sec. II.

II. DIS-SIMILARITY USING TEXTURE INFORMATION

From the density maps we can see the repetitions of the daily activity of residents. Tracking the change in periodicity of daily life is crucial for clinical purposes. A dis-similarity measure based on the co-occurrence matrix is proposed for evaluating differences in density maps. The average density and average time away from home can provide useful information on activity level of residents but cannot provide information about the periodicity of daily life. We propose to use texture information to provide this lifestyle periodicity information. The gray-level co-occurrence matrix (CM) is a statistical method which considers the spatial relationship of pixels and is often used for extracting textural features in images [10][11].

A. Co-occurrence Matrices of Images

The CM is derived from gray scale images. Suppose an image is rectangular and has N_x resolution cells in the

Manuscript received April 7, 2009. This work was supported by the National Science Foundation Grant IIS-0428420 and the Administration on Aging Grant 90AM3013/01.

S. Wang, M. Skubic are with the Electrical and Computer Engineering Department, Yingnan Zhu is with Computer Science Department, University of Missouri- Columbia, Columbia, MO 65211

horizontal direction and N_y resolution cells in the vertical direction. Suppose the gray scale value is quantized to N_m levels separately. Let $L_x = \{1, 2, \dots, N_x\}$ be the horizontal spatial domain, $L_y = \{1, 2, \dots, N_y\}$ be the vertical spatial domain, and $M = \{1, 2, \dots, N_m\}$ be the set of N_m quantized levels. The set $L_y \times L_x$ is the set of resolution cells of the image ordered by their row-column designations. The image can be represented as a function which assigns value M to each resolution cell or pair of coordinates in $L_y \times L_x$; $I: L_y \times L_x \rightarrow M$. An essential component is eight closely related measures from which all of the texture features are derived. These measures are arrays of adjacent or nearest-neighbor resolution cells. We consider a resolution cell to have eight nearest-neighbor resolution cells (Fig.2), excluding those on the periphery of an image.

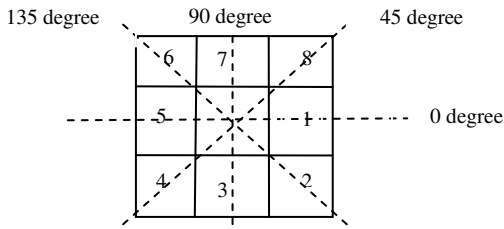


Fig.2. Resolution cells

The texture context information is specified by the matrix of relative frequencies P_{ij} with which two neighboring resolution cells separated by distance d occur on the image, one with gray level i and the other with gray level j computed as CMs. They are a function of the angular relationship between the neighboring resolution cells as well as a function of the distance between them. The CMs are defined in equation (1) [10]. Cardinality $\{S\}$ is the number of elements in set S . For the work presented here, $d=1$.

$$\begin{aligned}
 P(i, j, d, 0^\circ) &= \text{Cardinality}\{((k, l), (m, n)) \in (L_y \times L_x) \times (L_y \times L_x) \\
 &\text{where } k - m = 0, |l - n| = d, I(k, l) = i, I(m, n) = j\} \\
 P(i, j, d, 45^\circ) &= \text{Cardinality}\{((k, l), (m, n)) \in (L_y \times L_x) \times (L_y \times L_x) \\
 &\text{where } k - m = \pm d, l - n = \mp d, I(k, l) = i, I(m, n) = j\} \\
 P(i, j, d, 90^\circ) &= \text{Cardinality}\{((k, l), (m, n)) \in (L_y \times L_x) \times (L_y \times L_x) \\
 &\text{where } |k - m| = d, l - n = 0, I(k, l) = i, I(m, n) = j\} \\
 P(i, j, d, 135^\circ) &= \text{Cardinality}\{((k, l), (m, n)) \in (L_y \times L_x) \times (L_y \times L_x) \\
 &\text{where } k - m = \pm d, l - n = \pm d, I(k, l) = i, I(m, n) = j\} \\
 Q(i, j, d, a) &= \sum_a P(i, j, d, a)
 \end{aligned} \tag{1}$$

The CMs of activity density maps are calculated for comparison. The results will be shown in Section III.

B. CMs of Activity Density Maps

For a real application, computational speed is very important. The images of activity density maps must be generated first if the CMs are calculated from images directly. To avoid this step, we calculate CMs from the original data of density and TAFH, called the activity density map co-occurrence matrix (ACM).

The ACM is derived from the original density data and TAFH instead of images. The horizontal direction N_x of original data refers to 1440 minutes/day and the vertical direction N_y refers to the number of days. Each resolution

in the horizontal direction represents the density of a specific hour in that minute except the minutes away from home. Normally, the density per hour is lower than 550 per hour, so the density which is over 550 per hour is set to 550. The minutes away from home are set to a number larger than such as 750, which gives enough contrast to the maximum density. Suppose the density value is quantized to N_m levels separately. Let $L_x = \{1, 2, \dots, N_x\}, L_y = \{1, 2, \dots, N_y\}$ and $M = \{1, 2, \dots, N_m\}$. The original data D can be represented as a function which assigns value M to each resolution cell or pair of coordinates in $L_y \times L_x$; $D: L_y \times L_x \rightarrow M$. The ACM are defined similarly with equation (1).

C. Feature Extraction

1) Textural Features

All textural information is contained in the set of CMs. The equations which define a set of 14 measures of textural features are given in [11]. Due to the density map properties, the following subset of textural features is chosen:

$$f_1 = \sum_i \sum_j \{Q(i, j, d)\}^2 \tag{2}$$

$$f_2 = \sum_{n=0}^{N_x-1} n^2 \left\{ \sum_{i=1}^{N_x} \sum_{j=1}^{N_x} \sum_{|i-j|=n} Q(i, j, d) \right\} \tag{3}$$

$$f_3 = \sum_i \sum_j \frac{1}{1+(i-j)^2} Q(i, j, d) \tag{4}$$

$$f_4 = -\sum_i \sum_j Q(i, j, d) \log(Q(i, j, d)) \tag{5}$$

The angular second moment feature (ASM) (2) is a measure of homogeneity of the image. The contrast feature (3) measures the amount of local variations in an image. The inverse difference moment (4) also measures image homogeneity; this parameter achieves its largest value when most of the occurrences in the CM are concentrated near the main diagonal. Entropy (5) measures the disorder.

2) Other Features

Aside from textural features, there are two other features which are very important to discriminate the dis-similarity of density maps, average motion density per hour and average TAFH per day. These are used in the measurement also.

D. Investigating Different Distance Measures

The dis-similarity of two different density maps is represented by a number that is computed in feature space as the distance from one map to another. That is, the smaller the number, the more similar the density maps are. After generating the features of two density maps, we need to choose a distance measure to compare the difference. We experimented with 7 distance measures for comparison. In total, there are 6 features. Given a $1 \times m$ feature matrix x , which is treated as row vector $\{x_1, x_2, \dots, x_m\}$, the weighted normalized Euclidean distance d_{rs} between the vector x_r and x_s is defined as follows:

$$\begin{aligned}
 x_m(i) &= \frac{x_r(i)}{\max[x_r(i), x_s(i)]} \quad x_{sn}(i) = \frac{x_s(i)}{\max[x_r(i), x_s(i)]} \quad \text{for } i = 1 \dots 6 \\
 d_{rs} &= \sqrt{\left\{ \sum_{i=1}^6 w_i [x_m(i) - x_{sn}(i)]^2 \right\}} \quad \text{where } w_1, w_2, \dots, w_6 = \frac{1}{6}
 \end{aligned} \tag{6}$$

Features 5 and 6 are the average TAFH and the average motion density.

Different distance measures show similar trends in computing dis-similarity distance. For our purposes, the dis-similarities varying from zero to one are better for providing meaningful values to caregivers. In empirical results, the normalized Euclidean distance was shown to be the most sensitive and, thus, was chosen for the dis-similarity measure. Test results are shown in Section III.

III. RESULTS AND ANALYSIS

Due to the large set of data and limited space, only part of the comparison results are presented in this paper.

A. Single-Resident Results

Fig. 3 and 4 show the dis-similarity measure results for a resident using two distance measures. The density map of Jan., 2006 was compared to the other months (Fig. 5). Fig. 3 shows the comparison using Euclidean distance. The y-axis represents the distance in feature space and has two different scales for the different data sets. The solid purple line illustrates the dis-similarity of the ACMs using the Euclidean distance (using the right scale on the y-axis). The gray dashed line is the dis-similarity of the CMs (using the left scale on the y-axis). The dis-similarities of the image-based CMs and non-image-based ACMs follow a similar trend. The normalized Euclidean distance is shown in Fig.4 separately as it varies from zero to one. The solid purple line with empty circles illustrates the dis-similarity of the ACMs which uses 750 for TAFH and the other solid lines are 650, 1000 and 1500 values for TAFH. As expected the dis-similarity distance of the image-based CMs and the non-image-based ACMs follow a similar trend; the difference does not affect change detection.

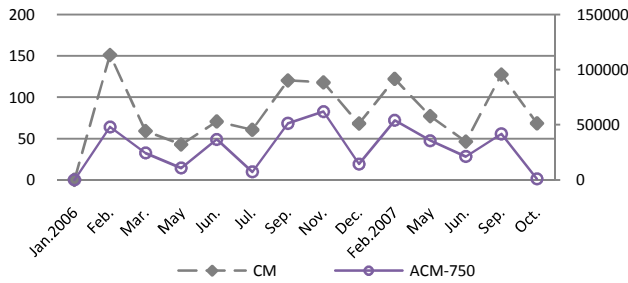


Fig.3. Comparison of Euclidean distance for one resident

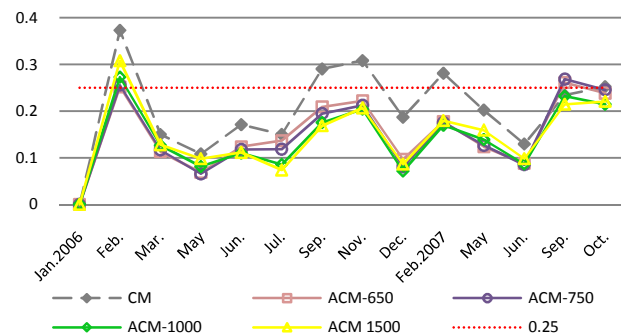


Fig.4. Comparison of normalized Euclidean distance for one resident

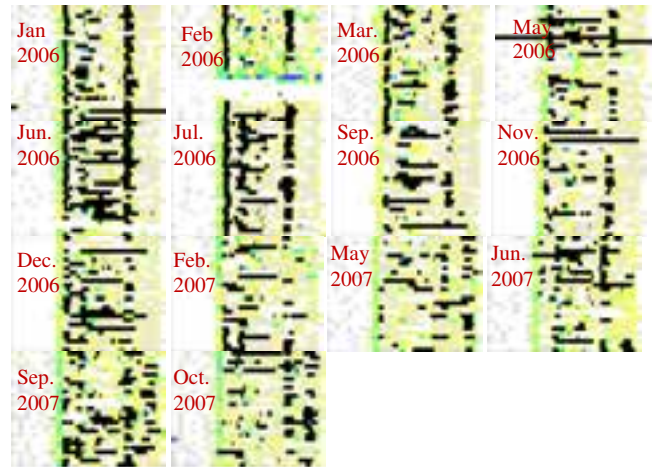


Fig.5. Density maps used for dis-similarity comparisons in Fig.3 & 4

B. Cross-Resident Results

Fig.6 shows the cross-resident dis-similarity results using normalized Euclidean distance. Residents 2-9 are compared to resident #1 (Fig.7). The dis-similarity distance of the image-based CMs and the non-image-based ACMs follow a similar trend in the cross-resident test.

There is an orange dashed line at 0.25 in both Fig.4 and Fig.6. For the single resident comparison (Fig.4), the dis-similarity measurements of normalized Euclidean distance of the ACMs are almost all smaller than 0.25. In contrast, for the cross-resident comparison (Fig.6), the dis-similarity measurements of normalized Euclidean distance of the ACMs are almost all larger than 0.25. The non-image-based ACMs give a better contrast between residents.

The solid lines in Fig.4 and Fig.6 are the comparisons of different values set for TAFH. We can see ACM 650, 750, 1000 and 1500 yield similar results in both figures, but when the value set for TAFH increases, the effect of density decreases. To place TAFH in a reasonable range, 750 is chosen as the value in the rest of the paper.

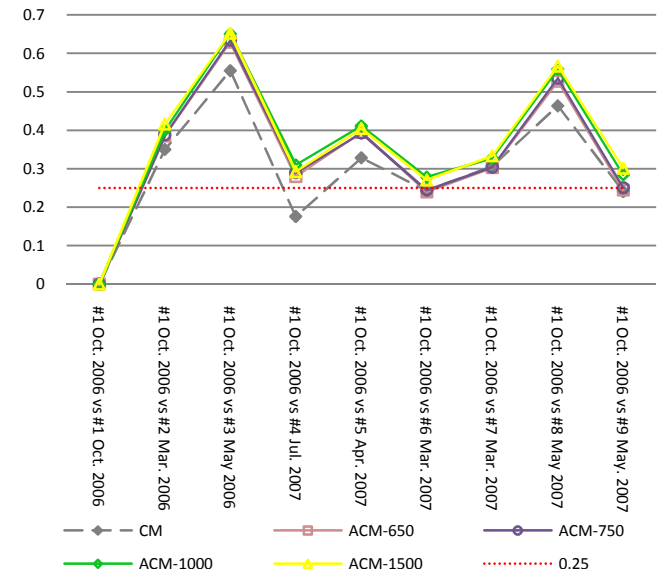


Fig.6. Cross-resident comparison of normalized Euclidean distance

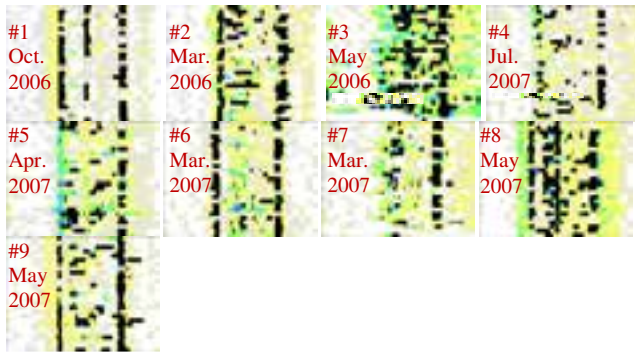


Fig.7. Density maps used for dis-similarity comparisons in Fig.5

C. Case Study

The dis-similarity measures were applied to data logged in the apartments of elderly TigerPlace residents. One case study is provided as an example of determining changes in activity patterns with the proposed method. In this section, the dis-similarity is computed using the normalized Euclidean distance based on ACM 750.

Fig.8 shows the dis-similarity measure results of the same resident. In this test, the density map Mar., 2006 is compared to other months (Fig.9). Fig.8 shows that the dis-similarity increases significantly after Mar. 2007. This indicates the activity level and the periodicity of life style of this resident varies from the original month Mar., 2006. This resident is #3 in Fig.7; we can see this resident has a dramatically different style of density map. The color is much darker than the others. She has a pattering style, and moves around the home more frequently. From Fig. 9, it can be seen that the color of density maps faded with time from Mar., 2006, and TAFH (the black area) decreased dramatically. These changes are consistent with the dis-similarity results.

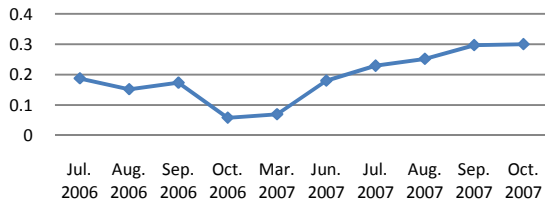


Fig.8. Dis-similarity changes of a resident

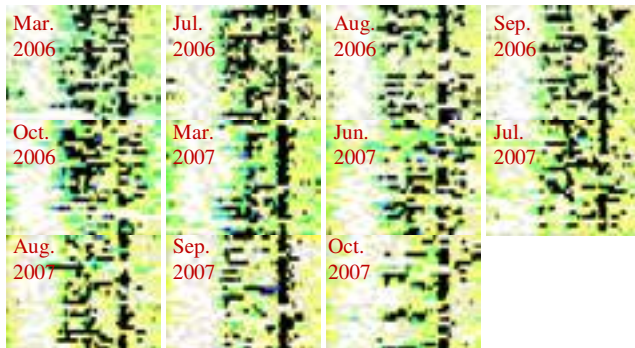


Fig.9. Density maps used for Fig.8

IV. CONCLUSION

Comparisons of density maps using the proposed dis-similarity measure are used to monitor the long term

activity level of older adults living at TigerPlace. The through dis-similarity measures provides an automated method for detecting changes in the patterns of residents that aids caregivers in the monitoring process.

However, there are limitations in the data analysis also. First, the motion sensor in the network cannot tag for personal identification. Thus, the decision made by the system will contain a degree of ambiguity to identify who performed the activity, and it is also a challenge to identify the number of persons in an apartment. Second, the motion sensor fires every 7 seconds if there is motion nearby, and useful information can be lost because of the 7 second resolution. On the other hand, the motion sensors used in this project are inexpensive and readily available. This kind of system is more easily affordable by a majority of older adults and is easy to deploy.

Our future research goals will expand on feature extraction and automated reasoning at different time scales using the logged sensor data, focusing especially on early detection of changes in patterns.

REFERENCES

- [1] KD Marek, MJ Rantz, RT Porter. "Senior care: making a difference in long-term care of older adults", *Journal of Nursing Education*, vol. 43; ISSU 2, pages 81-83, 2004
- [2] M. Skubic, G. Alexander, M. Popescu, M. Rantz, and J. Keller, "A smart home application to eldercare: current status and lessons learned," *Technology and Health Care*, in press.
- [3] K.Z. Haigh, L.M. Kiff and G. Ho. "Independent lifestyle assistant: lessons learned", *Assistive Technology*, 2006, vol. 18, pp. 87-106
- [4] R. Beckwith. "Designing for ubiquity: The perception of privacy", *Pervasive Computing*, April-June, 2003, pp. 40-46.
- [5] T.S. Barger, D.E. Brown, and M. Alwan. "Health-status monitoring through analysis of behavioral patterns", *IEEE Transactions on SMC-A*, vol. 35, no. 1, Jan., 2005, pp. 22-27.
- [6] N.M. Barnes, N.H. Edwards, D.A.D. Rose, and P. Garner." Lifestyle monitoring: technology for supported independence", *Computing and Control Engineering Journal*, Aug., 1998, pp. 169-174.
- [7] S. Brown, B. Majeed, N. Clarke, and B.-S. Lee. "Developing a well-being monitoring system- modeling and data analysis techniques", *Promoting Independence for Older Persons with Disabilities*, W. Mann and A. Helal, editors, Washington, DC: IOS Press, 2006.
- [8] C.D. Kidd, R.J. Orr, G.D. Abowd, C.G. Atkeson, I.A. Essa, B. MacIntyre, E. Mynatt, T. E. Starner and W. Newstetter. "The aware home: a living laboratory for ubiquitous computing research", *Proceedings of the Second International Workshop on Cooperative Buildings - CoBuild'99*, Position paper, October 1999
- [9] S. S. Intille, K. Larson, E. Munguia Tapia, J. Beaudin, P. Kaushik, J. Nawyn, and R. Rockinson, "Using a live-in laboratory for ubiquitous computing research", *Proceedings of PERVASIVE 2006*, vol. LNCS 3968.
- [10] B. Weyn, G. Van De Wouwer, M. Koprowski, A. Van Daele, K. Dhaene, P. Scheunders, W. Jacob, and E. Van Marck, "Value of morphometry, texture analysis, densitometry and histometry in the differential diagnosis and prognostic of malignant mesothelioma," *Journal of Pathology*, 1/01. 180, pp. 581-589, 1999.
- [11] A. Bemasoni, S. B. Antel, D. L. Collins, N. Bernasoni, A. Olivier, E Dubeau, G. B. Pike, E Andermann, and D. L. Arnold, "Texture analysis and morphological processing of magnetic resonance imaging assist detection of focal cortical dysplasia in extra-temporal partial epilepsy," *Annals of Neurology*, vol. 49, 2001.
- [12] S. Wang, M. Skubic, "Density map visualization from motion sensors for monitoring activity level", *Intelligent Environments, 2008 IET 4th International Conference*